Exploring the Evolution of Oxygen on the Early Earth: Constraining the Evolution of Oxidative Phosphorylation Through the Utilization of Uranium Isotopes

Christian N. Brown
Dr. Noah Planavsky, Advisor, First Reader
Dr. David Evans, Second Reader
29th April, 2015

A Senior Thesis presented to the faculty of the Department of Geology and Geophysics, Yale University, in partial fulfillment of the Bachelor's Degree.

Table of Contents

Abstract

The arrival of atmospheric oxygen onto the early Earth served as one of the most important events in evolutionary history as it fundamentally altered all biological organisms and pathways. Despite its importance, however, the exact time period in which atmospheric oxygen arose prior the Great Oxidation Event (GOE) is heavily contested, despite the GOE occurring roughly 2.3 to 2.5 billion years ago. It has been hypothesized that the GOE resulted as a response to the rise of oxygenic photosynthesis, but this evolutionary adaptation has also been hard to

chronologically constrain. Previous methods attempting to constrain the rise of oxygenic photosynthesis through biomarkers has proven to be inaccurate and unsuccessful. Novel isotopic systems, such as uranium ($^{238}U/^{235}U$) expressed as $\delta^{238}U$, can be used to express redox conditions that serve as proxies for oxygen levels on the early Earth. Through this study in the Pongola supergroup (>2.95 million years), the Barberton group (3.55-3.22 billion years), and the Animike group (2.5-1.8 billion years), the rise of oxygenic photosynthesis can be further constrained within distinct time periods in the Archean. Here, initial findings suggest the presence of oxygen caused by oxygenic photosynthesis through redox conditions in some sections of the Pongola group. Through this, it is inferred that oxygenic photosynthesis must have been present in local settings for a significant period of time prior to the GOE. However, the collection of additional data points is required to ascertain the validity of this claim.

Introduction

1. Oxygen Arrival on the Early Earth

Oxygen is arguably one of the most important elements on Earth as it governs all modern biological processes. From modern human respiration to the oxygen that facilitated the megafauana, oxygen currently has and continues to play arguably the most influential role in the environment. Yet in Earth's greater history this was not always the case. For a significant portion of time in Earth's history, the entire planet was in an entirely anoxic state and only through an event during the Archean known as the Great Oxidation Event (GOE) was it able to change (Holland, 2006). Based on dating provided from Banded Iron Formations, the GOE was said to have occurred roughly 2.3 billion years ago (Ibid.). It is following this shift from an anoxic world to an oxygenic one that majorly altered all evolutionary life pathways.

The exact cause and timing of the rise of the GOE is extremely opaque however, and various theories have emerged on the origin of this event. The leading hypothesis on this rise in atmospheric oxygen levels is that development of cyanobacteria occurred near this time period of the GOE at 2.3 Ga (Ibid.). These cyanobacteria were then thought to have produced a large enough amount of oxygen through oxygenic photosynthesis that they then shifted the Earth from its anoxic state to its oxygenic one.

The exact timing of this, however, is largely debatable depending on the type of marker that is being used. As shown on Figure 1., a variety of different techniques have had limited success in attempted to constrain the rise of oxygenic photosynthesis. Historically, biomarkers were used to determine the rise of these bacteria, however, recent evidence has shown that there may be significant experimental flaws associated with the findings of these biomarker studies (Wang 2014). Additionally, paleontological records have been used to attempt to track the rise of photosynthesis but these have also been proved to be insufficient.

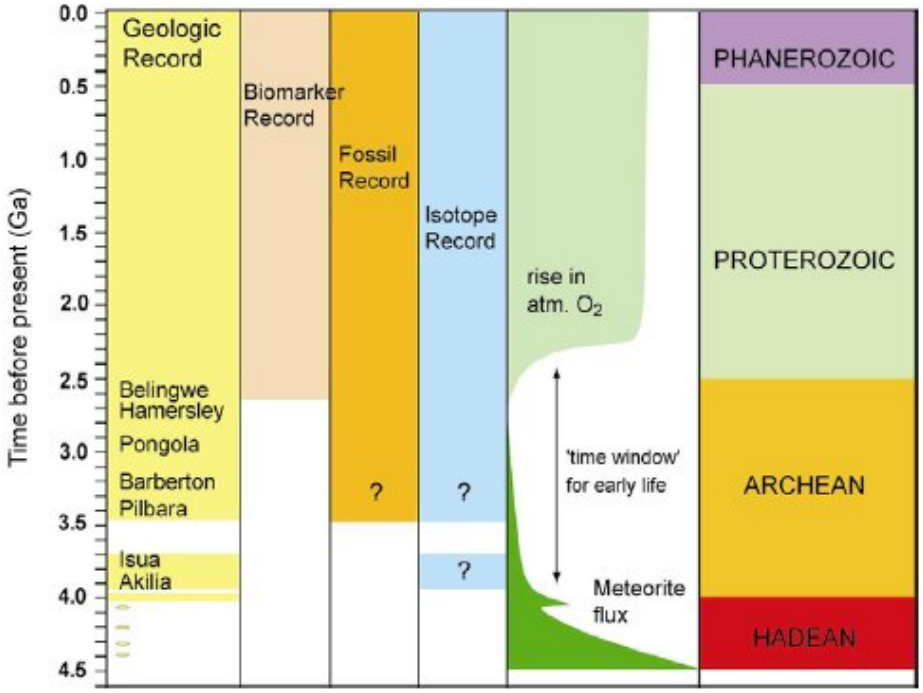

Figure 1. Oxygen Concentration Versus Various Geological Markers

(Mark Van Zuilen, IGPG, 2006)

Isotopic records as a response to reduction-oxidation conditions instead to seem to be the most confident way to attempt to constrain the period in which oxygenic photosynthesis could have developed. Through the use of mass-independent fractionation of sulfur isotopes, Holland speculates that in the Archean, oxygen levels would have likely been roughly 10^5 times less than current oxygen levels (Ibid.). There is some error in this, however, that occurs with the mass-independent fractionation of sulfur isotopes from the period of 3.0 to 2.8 billion years ago. Here there appeared to be a change in atmospheric conditions as the sulfur isotope changes from a non-zero value to a small negative value (Ibid.). Holland's interpretation was that this was caused by a decrease in all atmospheric gases from some unknown cause, and this discrepancy in the rock record was able to correct itself by 2.45 billion years ago (Ibid.). This anomaly, although only present in sulfur, is also something that must be considered in all samples during these time periods.

2. Evolution of Oxygenic Photosynthesis

One of the main stresses by Holland is that there is a lack of information towards total atmospheric oxygen during this time period in not only the rock record but the evolutionary biological record as well. One of the most current view of the evolution of photosynthesis through 16S rRNA constructions of phylogenetic relatedness of photosynthetic gene sequences in modern bacteria is that photosynthesis evolved in very non-linear manner (Mulkidjanian et.

Al.). It has been thought that photosynthesis initially started as a metabolic process that existed entirely under anoxic conditions (Ibid.). Because there was not a significant presence of oxygen in the atmosphere the sun's light was much harsher on the surface of the Earth (Ibid.). Some scientific groups have proposed that in response to this, oxygenic photosynthesis evolved under incredible selective pressure as a method to both incorporates this sunlight into the metabolism as well as to protect themselves from these intense rays of sunlight (Ibid.). From this, a metabolism that generated oxygen was developed but the evolution of this process is not well understood.

From the sulfur isotope record it is clear that atmospheric oxygen "seems to have appeared irreversibly between 2.41 and 2.32 Ga." (Holland). Here, there appears to be a spike in the mass independent sulfur isotope record that does not return to the relatively zero position that it had maintained for major portions of the Archean. This event is coupled with a global halt in the development of banded iron formations that lasts roughly three million years (Ibid.). This period over which this occurs, roughly 2.4 to 2.0 billion years ago is referred to as the Great Oxidation Event, and is additionally marked by changes in the carbon isotope values with a positive excursion (Ibid.). From this point onwards, the composition of the rock record is dramatically altered as all of the sulfide and iron molecules begin to be changed into their oxidized forms. Using this same principles as Holland completed with the great oxidation event, previous events marking the evolution of oxidative photosynthesis can be viewed, and specifically this thesis uses uranium isotopes as opposed to sulfur to accomplish this.

2. Uranium Isotope System

Uranium isotopes are one of multiple systems currently involved in tracking the development of oxygenic photosynthesis and it serves as a very unique system compared to other isotopic techniques. First of all, uranium is a much heavier element with an atomic number of 92. This element lies in the actinide series and is entirely composed of radioisotopes as opposed to being made of stable isotopes. Traditionally, uranium isotopes have been utilized in methods of dating with uranium-lead based systems. However, this research seeks not to utilize the decay of uranium as much as the uniqueness of the element. Uranium is unique in the fact that although it has six reduction-oxidation states, only two of these states are primarily utilized, those being uranium (VI) and uranium (IV) (Partin et. Al.).

These states are notable as uranium (VI) only occurs in an insoluble solid form, while uranium (IV) occurs in a dissolved soluble form (Wang). Through the change in oxidation states of uranium a fractionation even occurs that serves as a marker of ocean oxidation state (Ibid.). Uranium (VI) largely occurs in crustal environments, and only through interactions with solution (water) can it be freed from this into a basin. Figure 2., largely descries the possible methods in which uranium is removed from parent rock into solution.

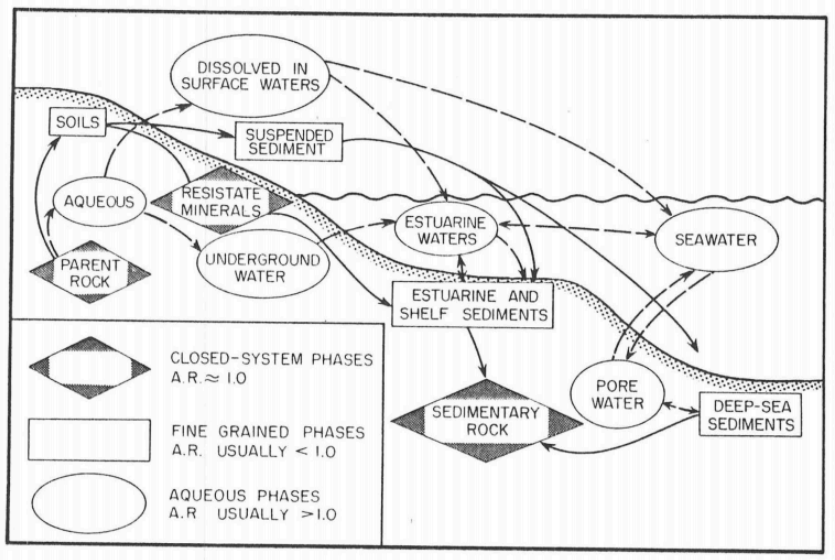

FIG. 24. Geochemical cycle of uranium near the earth's surface. Disequilibrium is initiated by water-mineral interactions in soils and weathered rock, and in aquifers where the surface to volume ratio is high. In general, a fine grained solid phase will exhibit $^{234}U/^{238}U$ activity ratios less than 1.00 due to grain surface leaching and/or alpha recoil. Aqueous phases, including groundwater, surface water and ocean water, generally exhibit ratios greater than 1.00. In some parts of the cycle, e.g. soils, seawater and sediments, the uranium residence time is long enough so that the decay of ^{234}U, with a half-life of 250 thousand years, can affect the A.R.

Figure 2. Methods of Uranium Transport (Osmund and Cowart)

Additional fractionation occurs between the change of the redox states. The reduction from uranium (VI) to uranium (VI) is relatively low in the affect that it has on fractionation, while the oxidation of uranium (IV) to uranium (VI) has a relatively high impact on oxidation. Additional kinetic factors also occur because uranium is rarely found in the crust. In comparison to this, however, uranium is found at abnormally high concentrations in seawater where it is unable to buried back into sediment at the same rate that it is leached out (Ibid.). This creates a disequilibrium in the system that then allows uranium to be tracked where there is much more uranium should be possible from a mass balance perspective dissolved in seawater (Partin). Additionally, uranium is additionally not produced by hydrothermal systems so this gives uranium that has been deposited in sediments a very unique and descriptive property that is not entirely shared among other isotope systems (Ibid.). Only the uranium that is being measured

from the direct run off from crustal sediment is largely measured through isotopic fractionation, whereas other systems could be heavily impact as they move towards their depositional environment.

With this framework in mind, scientists such as Partin et al. have measured uranium concentrations from various rocks from the modern to the Archean and have slowly pieced together the story of the development of the Great Oxidation Event and the development of atmospheric oxygen through the use of the 238U/235U ratio (Ibid.). This can be accomplished, as uranium is a radioisotope and there is very little contamination that occurs of it in nature. This also allows for isotopes of uranium to be very efferent in the environment, with very small existence. When uranium is compared for fractionation, it is done through the ratio described below from Weyer et. Al, 2008 (Weyer et. Al., 2008).

$$\delta^{238}U = \left[\frac{(^{238}U/^{235}U)_{sample}}{(^{238}U/^{235}U)_{standard}} - 1\right] \times 1000$$

Large isotopic fractions can only be assumed to have occurred through significant chemical alterations, as presented in research done by Weyer et. Al. and represented in Figure 3 (Ibid.). These chemical changes are primarily facilitated through microbial mediation, and this can be described below through the different eventual deposition environments corresponding to the values of fractionation. The heaviest of the values occur in black shales where the lightest of the values occur in ferro-manganese deposits (Ibid.). Using this framework, if isotopic fractionation values differ significantly from 0.3±0.1 ppm, it can be confidently assumed that there is evidence for redox conditions that are affecting samples as a result of oxygen. This can then be inferred forward that this would be a potential indicator of the development of oxygenic photosynthesis.

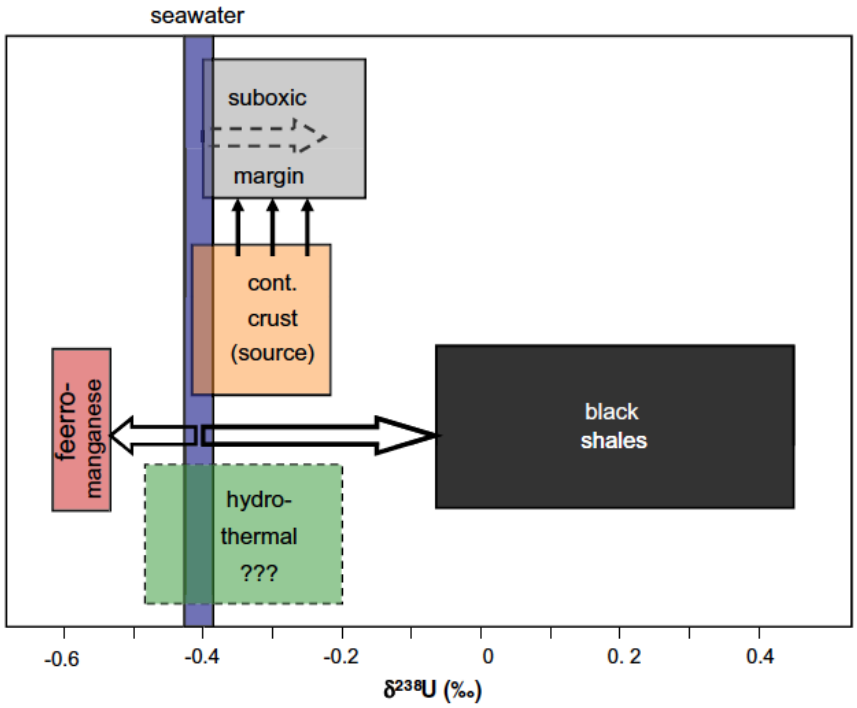

Figure 3. Fields of Fractionation of Natural U Isotopes (Wayer et Al., 2008)

Study Area

The samples used throughout this experiment were from three primary localities. All three of these localities are geographically separated but all represent large stretches of geological time during the Archean time period. These locations were chosen primarily for the fact that they could be used comparatively against each other through geological time periods. These include the Pongola supergroup, the Barberton greenstone belt, and samples from the Animikie basin.

The samples from the Pongola supergroup are formed from succession of rocks in the Kapvaal Craton in South Africa (Young et Al. 1998). These supercrustal rocks are dated at roughly 2.9 billion years old, and sit on top of granites dated at 3.1 billion years (through U-Pb dating) (Ibid.). The Ponogla formation is primarily created from alternating sections of basalts,

sandstomes, and limestones, and has undergone low-grade metamorphism into green-schist (Ibid.). Visually, these samples were largely red, iron rich sediments that were tested.

The samples that come from the Barberton supergroup serve as the oldest samples among the three that were viewed. The Barberton Greenstone Belt covers between 3.2 to 3.5 billion years of time in the Barberton group within the Transvaal Providence of South Africa (Kroner et Al, 1996). In this study, specifically the Fig Tree Formation (~3.26 Ga) was looked at as part of the Barberton Drilling Project (Ibid.). The Fig Tree Formation, is primarily composed of alternating layers of ferruginous cherts and banded iron formations. Visually, these samples were primarily darker sediments compared to the vibrant Pongola samples.

The final samples viewed were part of the Animikie formation, located in the Lake Suprerior Region and dated to roughly 1.88 billion years old (Planavsky, 2008). This formation is created from a depositionally diverse set of iron rich successions and is constrained by volcanic successions and the Gun Flint range (Ibid.). These samples were used to provide a much younger viewpoint to check the other two samples against. Visually, these were dark grey and brown samples.

Materials and Methods

1. Preparation for Trace Metal Analytical Methods

All of the materials and samples using in this project were collected through Noah Planavsky. Prior to experimentation all samples were obtained as mechanically powdered from their original solid form. These included samples from the Barberton IV group (labeled BBT), the Pongola group (labeled PG), and a second batch of Pongola group samples in addition to Animikie group samples (labeled PA).

Prior experiments determined the amount of sample that needed to be used in this experiment in order to obtain a quantifiable amount of uranium through mass spectrometry. In the case of both the Pongola (PG) samples, between 0.30 grams and 0.40 grams were dissolved for 28 PG samples. For the Pongola/Animikie samples, roughly 0.40 grams were dissolved for 20 PA samples. For the Barberton (BBT) samples, it was previously found that the mass spectrometer would be unable to detect uranium when small amounts of the samples were digested. As a response to this, 2.0 grams of sample were digested for 23 BBT samples, as opposed to the significantly smaller mass in the other samples. For all samples, four standards were used, including two USGS Manganese Nodule geostandards, Mn-A-1, were used as well a two USGS Hawaiian Basalt, BHVO-2. Two duplicates of samples were also made in each data set to ensure reliability of the samples. Additionally, two blanks were created for each sample set to monitor the quality of the Clean Lab conditions.

2. Silicate Digestion

All of the silicate digestion methodology followed the Standard Operating Procedure (SOP) created by Xiangli Wang. The primary goal of the digestion was to free the uranium from the bonds present within the powdered rock samples. After all samples were weighed, they were placed into Teflon beakers. To the beakers, 2 mL of concentrated nitric acid (HNO_3) was added to the samples. Following this 0.4 mL of concentrated hydrofluoric acid (HF) for every 100 mg of sample was added. Because of the size of the BBT samples, this was completed in multiple parts to ensure safety with the HF and to minimize a large, exothermic reaction as well as the creation of silicon tetrafluorides gases (SiF_4). Following this the Teflon beakers were caped and placed on a hot plate at 100 degrees Celsius for a full day. The cap was then removed and the

Teflon beakers were then left to evaporate to dry at 100 °C for another full day. Following this, 2 mL of 6 N hydrochloric acid (HCL) were then added to the beaker with the addition of 2 mL of 6 N HNO_3 . The beakers were then caped and placed on a hot plate at 100 °C for a full day. Following this, the cap was then removed and the Teflon beakers were then left to evaporate to dry at 100 °C. Next 4 mL of 6 N HCL were then added to the samples again, caped, and placed on the hot plate at 100 °C for another full day. These were then uncapped and dried at 100 °C for an additional day. After this the samples were then raised in 4 mL of 6 N HCL and transferred from their original beakers to 4 mL plastic tubes.

3. Uranium Column Methodology

Following the digestion of the samples, the samples were then dried down. They were then double spiked with a 2 ppm In spike in HNO_3 solution depending on both the original amount of sample and the uranium concentration of the sample obtained from previous experiments. The goal of this was then to obtain 100 ng of uranium to be detected in the mass spectrometer. Once spiked the samples were dried down another time. The double spike samples were then raised in 5 mL of 3 M HNO_3.

The next uranium column methodology comes from Xiangli Wang. Following this, 0.8 mL of UTEVA resin was used to fill premade columns. Through the columns, 0.05 N HCL was used to fill and clean the reservoir. After this an additional 2 mL of 0.05 N HCL was used to also clean the column. From this, the column was then conditions with 2 mL of 3 N HCl. The samples were then loaded into the columns. The matrix was then eluted by adding 6 mL of 3 N HNO_3 twice. The thorium was then removed form the UTEVA resin by adding 2 mL of 10 N HCl followed by 4 mL of 5 N HCl twice. Finally, the uranium ions were collected by adding 5

mL of 0.05 N HCl twice. The columns were then cleaned and the sample were dried on a hot plate at 100 °C for a full day. Following this, a single drop of HNO_3 was added to condition the sample and then these were dried down completely. Finally the samples were raised in 4 mL of HCl and prepared to be sent through the mass spectrometer.

4. Uranium Isotope Detection

Following the uranium collection methodology, the samples were then run through the Neptune Plus High Resolution Multicollector ICP-MS. All of the collection of data and isotope values was obtained through the help of postdoctoral student Xiangli Wang. The results of which are available in the three appendices attached at the end of the thesis.

Results

Three different plots were created from the different localities based on the isotopic fraction of $\delta^{238}U$ for the different samples.

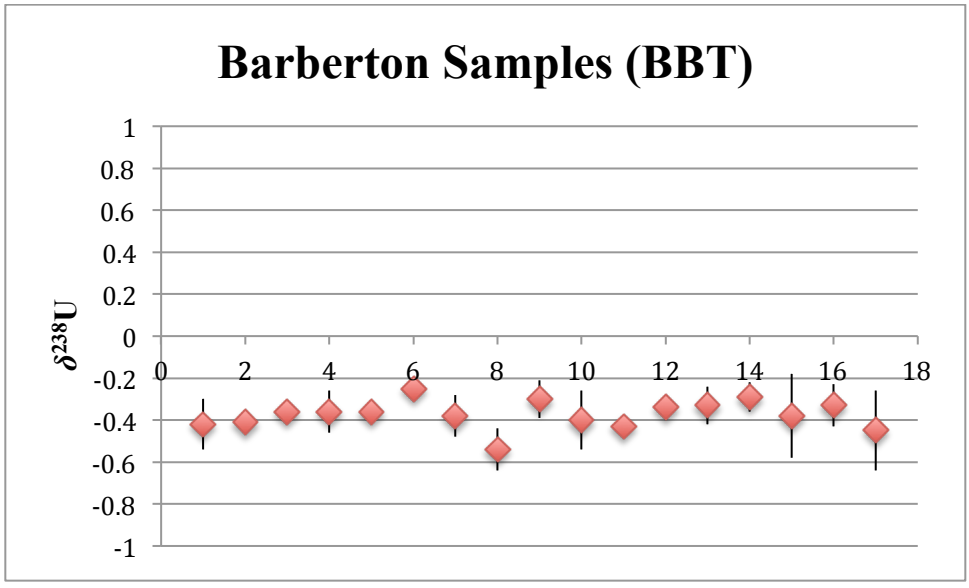

Plot 1. Barberton δ^{238}U Fractionation

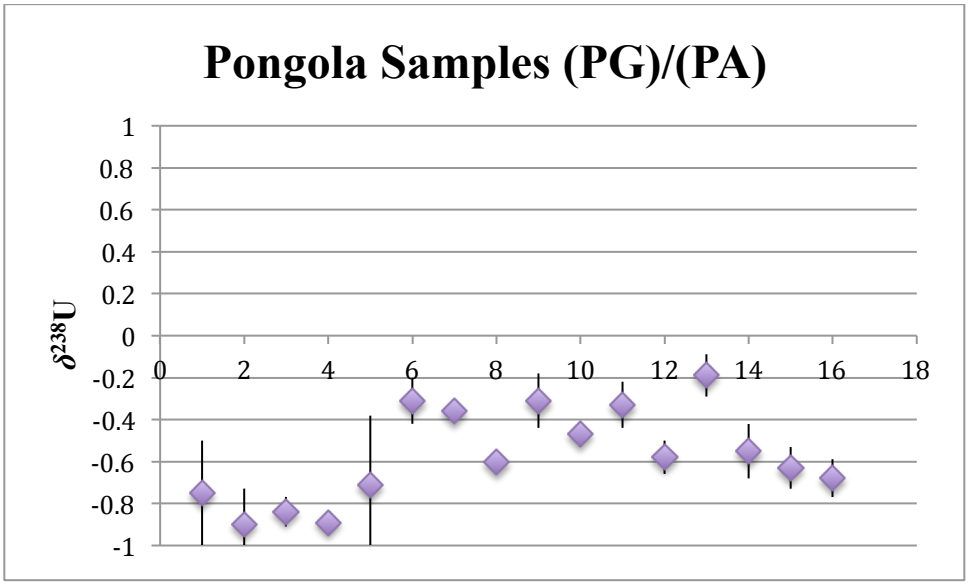

Plot 2. Pongola δ^{238}U Fractionation

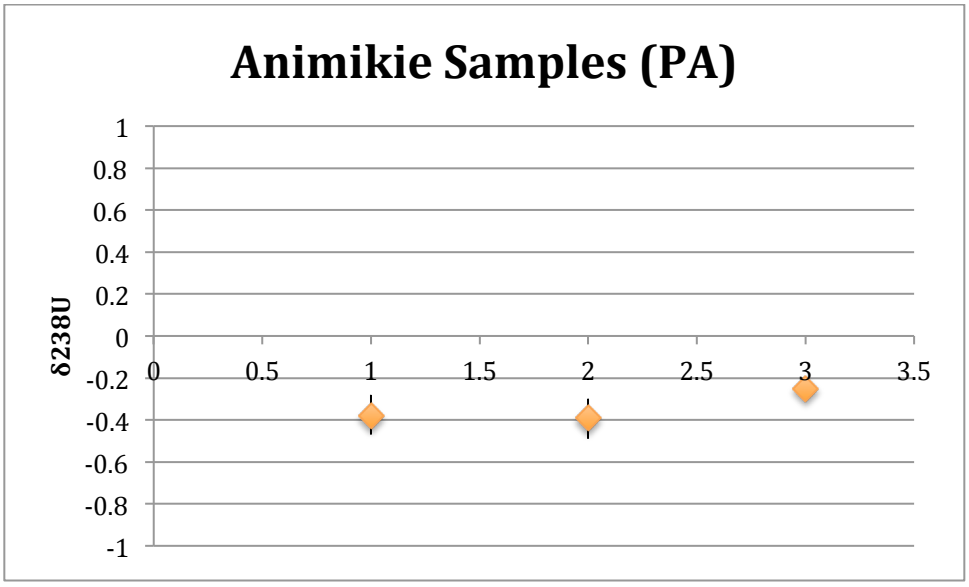

Plot 3. Animikie δ^{238}U Fractionation

An additional two figures were obtained from Xiangli Wang, including data from the same locality. These data points were to be used to compare against the data collected as a part of this thesis.

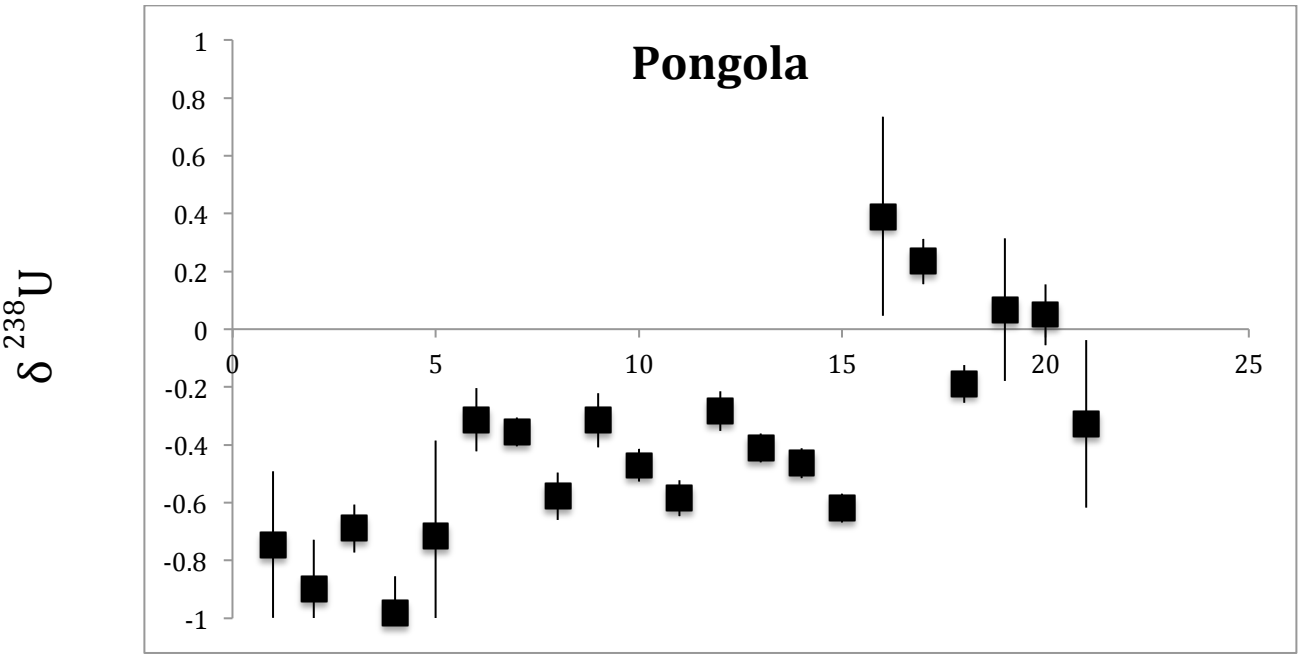

Plot 4. Pongola δ^{238}U Fractionation from Xiangli Wang

Discussion

From the data obtained both through the experiment preformed as well as from postdoctoral student, Xiangli Wang, there appeared to be a clear correlation with the δ^{238}U fractionation among some samples and not others. Specifically, the animikie group and the Barberton greenstone belt seemed to all -0.3 ppm, something that would be expected from the background fractionation of uranium (Plot 1 and Plot 3). In contrast to this, however, the Pongola samples seem to be both enriched as well as depleted compared to the background rate. This gives rise to values of as high as +0.4 ppm and as low as -1.0 ppm in the Pongola samples (Plot 2

and Plot 5). From this, and previous research, it can be assumed that this is a possible indicator of oxygenic photosynthesis as the values present the possibility of redox conditions causing this change in fractionation.

When compared to other measurements taken by the Planavsky laboratory, these results appear to be consistent with general trends. As presented in Figure 4.. the Barberton Fig Tree Group appears to not experience any deviation because of a lack of oxygen presence. In comparison to this, however, the Pongola supergroup is much more reflective of the modern environment as a result of having redox conditions influenced by oxygen. This is consistent with the findings of the study preformed in this thesis.

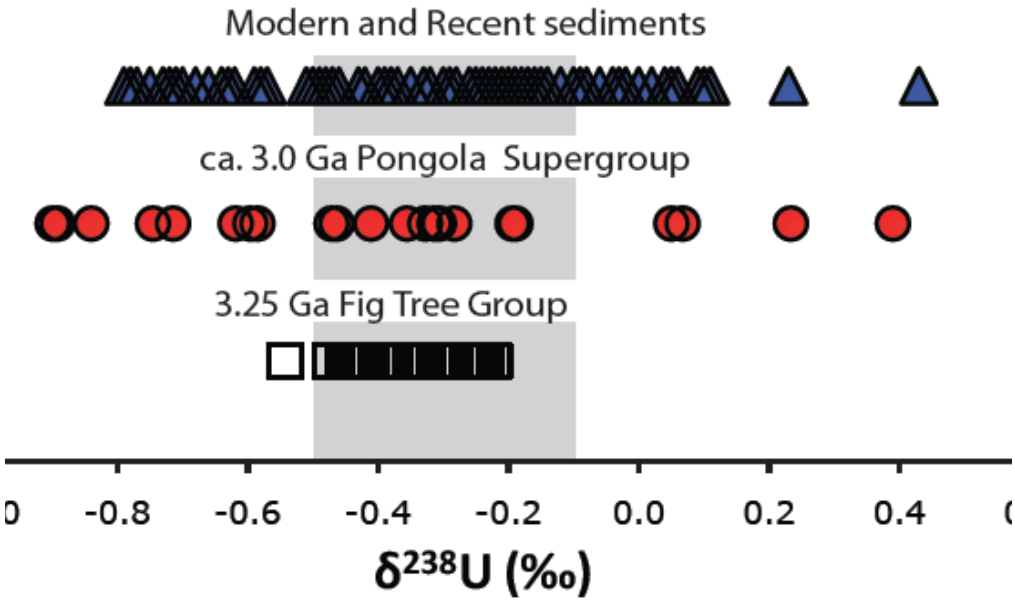

Figure 4. Comparison of Barberton (Fig Tree Group) and Pongola Samples to Modern Sediments (Planavsky, *unpublished*)

This is also consistent with other isotopic data. Sulfur isotopes present an early anomaly or "burp" around 2.6 billion years ago that was thought to be representative of an earlier

evolution of oxygenic photosynthesis (Holland, 2006). Additional studies in molybdenum isotopes have also presented the possibility of manganese oxides being formed in Pongola sediments elsewhere in the Pongola supergroup at 2.9 Ga (Planavsky et Al., 2014). Here, oxygen once again is thought to have played a role within the fractionation and this helps to support the idea that oxygenic photosynthesis arose prior to the GOE at 2.3 Ga.

Related molecular clock data also shows an earlier time for the evolution of oxygenic photosynthesis compared to what was viewed original through the use of biomarkers. As presented in figure 5., when the mutation rates of certain genes related to oxygenic photosynthesis are calculated backwards, there appears to be a large amount of activity around 3.0 Ga, compared to the 2.3 Ga thought to be associated with the Great Oxidation Event (David and Alm, 2011). This provides further proof of the legitimacy of the Pongola samples being representative of oxygenic photosynthesis, and this possibly being more influential than a local event.

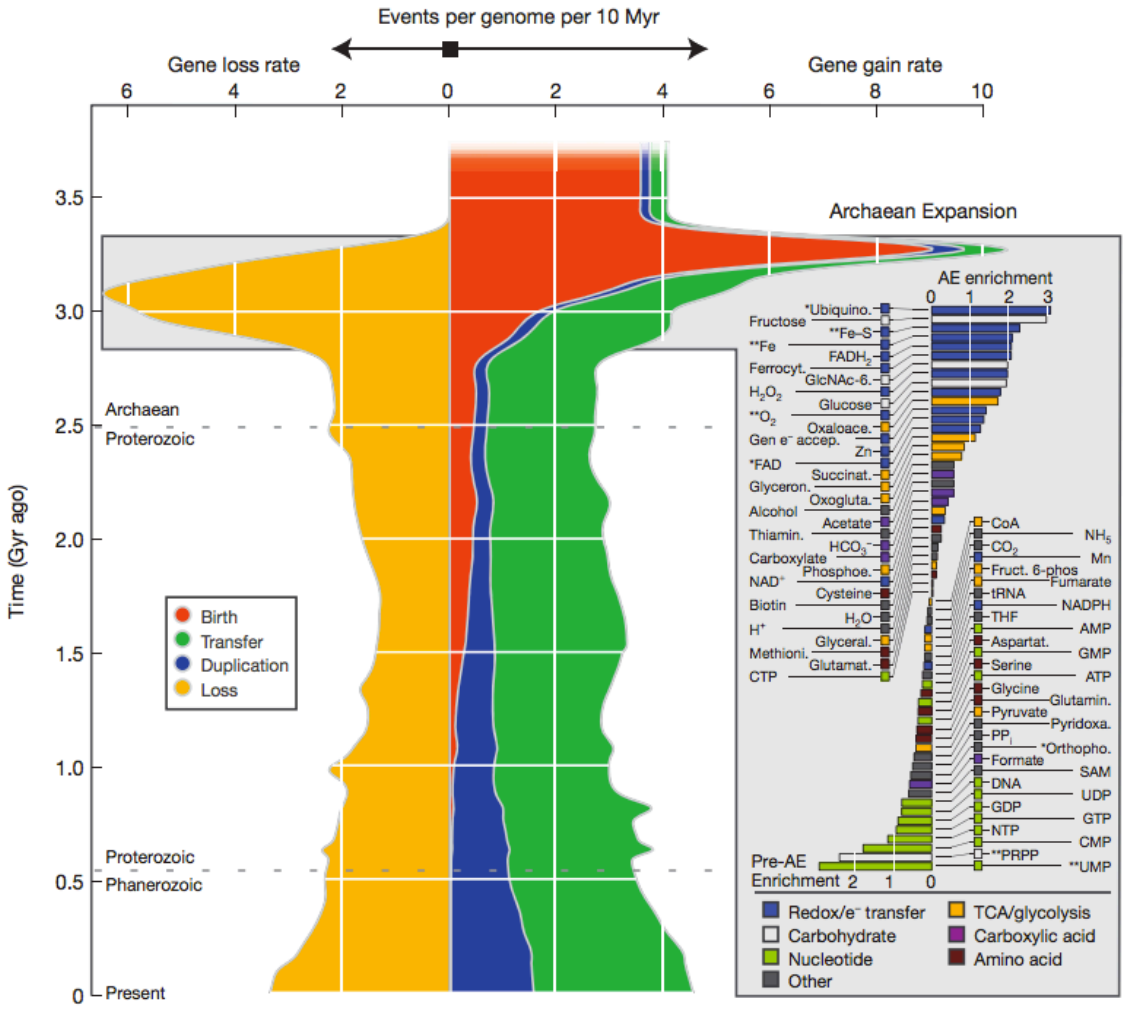

Figure 5. Molecular Clock Evidence for Oxidative Photosynthesis Development (David and Alm, 2011)

Conclusion

This study set out to determine if it would be able to better constrain the development of oxygenic photosynthesis through the use of uranium isotope fractionation in the Pongola supergroup, the Barberton Greenstone belt, and Animikie group. There appeared to be no significant deviation from background fractionation in either the Barberton Greenstone belt or the Animikie group that would suggest that there were significant levels of oxygen in the

atmosphere. However, the Pongola supergroup showed deviation away from the background levels in both enriched and depleted directions in both the samples ran through this thesis as well as independently by Xiangli Wang. These results suggest that there was at least isolated oxygen in the Pongola supergroup, possibly as a result of oxygenic photosynthesis. Additional samples need to be taken to ensure that this is not merely an isolated effect, however.

Future Study

Although numerous samples were processed throughout the course of research over the past two years, including multiple sets of data not included in the thesis, additional research still needs to be done in certain areas. Specifically, the Animikie supergroup data should be increased to more than three data points. Also, when this project was first started the two isotopes that were to be used were chromium and uranium. Chromium, however, has both a longer and more technical column ion removal process than does the uranium method. With more time, additional data sets could be created with the chromium isotope method that should be used to support the rise of oxidative photosynthesis through an additional proxy. Finally, this research would also be useful in an interdisciplinary setting where the uranium data could be used and compared to the molecular clock of genes present in the development of photosynthesis, so that the results of these studies could be used to support each other.

Acknowledgements

Thank you to my thesis advisor, Professor Noah Planavsky, for helping me through everything I did throughout this research process. Additionally thank you to Postdoctoral student

Xiangli Wang, for helping me with all of the laboratory techniques and advising through this entire research process. Thank you to mentor, friend, academic advisor, and Director of Undergraduate Studies for Geology and Geophysics Professor David Evans. Finally that you to the other members of the Planavsky Laboratory, including both Ying Kui and Huijuan Zou for teaching and helping me with everything that I have done in the with Yale Clean Laboratory. Finally, thank you to the faculty, staff, and graduate students of the Geology Department for providing me with an amazing four years and fundamentally shaping my Yale experience. Additional thanks to the Pierson College: Richter Fellowship, the Von Damm Class of '77 Fellowship, and the Yale College Dean's Research Fellowship.

References Cited

Bekker, A. et al. 2004. "*Dating the rise of atmospheric oxygen.*" Nature. Volume 427. pp. 117–120.

David and Alm. 2011. "*Rapid evolutionary innovation during an Archaean genetic expansion*." Nature. Letters. Volume 469. p. 93-96.

Holland, Heinrich D. 2006. "*The oxygenation of the atmosphere and oceans.*" Philosophical Transactions of the Royal Society: Biological Sciences. Vol. 361. 2006. p. 903–915.

Kroner et Al. 1996. "*The oldest part of the Barberton granitoid-greenstone terrain, South Africa: evidence for crust formation between 3.5 and 3.7 Ga*." Precambrian Research. Volume 78. p. 105-124.

Johnson et. al. 2013. "*Manganese-oxidizing photosynthesis before the rise of cyanobacteria*" PNAS. Volume 110, number 28. Pp. 11238-11234.

Johnson et. Al. 2014. "*O_2 Constraints from the Paleoproterozoic detrital pyrite and uranite.*" Geological Society of America Bulletin. P. 1-18

Konhauser et. Al. 2011. "*Aerobic bacterial pyrite oxidation and acid rock drainage during the Great Oxidation Event.*" Nature. pp. 369-374

Mulkidjanian et. Al. 2006. "*The cyanobacterial genome core and the origin of photosynthesis.*" PNAS. Volume 103, number 5. p. 13126-13131.

Osmond and Cowart. 1976. "*The theory and uses of natural uranium isotopic variation in hydrology*." Atomic Energy Review, Issue 14, Volume 4. p. 621-679.

Partin et. Al. 2013. "*Large-scale fluctuations in Precambrian atmospheric and oceanic oxygen levels from the record of U in shales."* Earth and Planetary Science Letters. Volume 369, pp 284-293.

Planavsky et Al. 2009. "*Iron-oxidizing microbial ecosystems thrived in late Paleoproterozoic redox-stratified oceans."* Earth and Planetary Science Letters. Volume 286. pp. 230-242.

Wang et Al. 2014. "*Low Mid-Proterozoic atmospheric oxygen levels and the delayed rise of animals*." Science. Volume 346, number 6209. pp. 635-638.

Wang et Al. 2014. "*Uranium Isotopes and Archean Oxygen Levels*." *In Review.*

Weyer et Al. 2008. "*Natural Fractionation of 238/235U*." Geochimica et Cosmochimica Acta. Volume 72, Issue 2. P. 345-359.

Young et Al. 1998. "*Earth's Oldest Reported Glaciation: Physical and Chemical Evidence from the Archean Mozaan Group (~2.9 Ga) of South Africa*." The Journal of Geology. Vol. 106, No. 5. pp. 523-538.

Appendix

Table 1. Barberton Samples (BBT)

Analysis Code	Sample Name	$\delta^{238}U$	2StdError
BBT-1	BHVO	-0.26	0.10
BBT-2	BHVO	-0.20	0.08
BBT-3	Mn Nodule	-0.51	0.06
BBT-4	Mn Nodule	-0.63	0.06
BBT-6	261.63	-0.42	0.12
BBT-7	317.69	-0.41	0.05
BBT-8	277.81	-0.36	0.05
BBT-9	304.08	-0.36	0.10
BBT-10	422.83	-0.36	0.05
BBT-11	317.69	-0.25	0.05
BBT-12	304.08	-0.38	0.10
BBT-14	354.7	-0.54	0.10
BBT-15	277.81	-0.30	0.09
BBT-16	363	-0.40	0.14
BBT-17	277.81	-0.43	0.05
BBT-18	314.95	-0.34	0.05
BBT-19	264.49	-0.33	0.09
BBT-20	316.14	-0.29	0.07
BBT-21	299.17	-0.38	0.20
BBT-22	285.06	-0.33	0.10
BBT-23	240.23	-0.45	0.19

Table 2. Pongola Samples (PG)

Analysis Code	Sample Name	$\delta^{238}U$	2StdError
PG-5	PG-5C	-0.75	0.25
PG-6	PG-6C	-0.90	0.17
PG-7	PG-4	-0.84	0.07
PG-11	PG-3	-0.89	0.05
PG-12	166.6	-0.71	0.33
PG-13	166.4	-0.31	0.11
PG-14	PG-6	-0.36	0.05
PG-15	167-167.1	-0.60	0.05
PG-17	170.1	-0.31	0.13
PG-18	167-167.1	-0.47	0.06
PG-23	BHVO2	-0.19	0.06
PG-24	BHVO2	-0.16	0.09
PG-25	Mn Nodule	-0.72	0.05

Table 3. Pongola and Animikie Samples (PA)

Analysis Code	Sample Name	$\delta^{238}U$	2StdError

PA-2	317-8	-0.33	0.11
PA-3	PG-5a	-0.58	0.08
PA-7	DH3-42	-0.38	0.09
PA-8	317-16	-0.19	0.10
PA-9	DH3-43	-0.39	0.10
PA-11	317-26(NP8)	-0.55	0.13
PA-13	317-20	-0.63	0.10
PA-15	MS4C(2)	-0.25	0.05
PA-17	PG5-A	-0.68	0.09
PA-19	BHVO-2	-0.36	0.09